

# Recognition in Unseen Domains: Domain Generalization via Universal Non-volume Preserving Models

Thanh-Dat Truong<sup>1</sup>, Chi Nhan Duong<sup>2</sup>, Khoa Luu<sup>3</sup>, Minh-Triet Tran<sup>1</sup>

<sup>1</sup> University of Science, VNU-HCM, Vietnam

<sup>2</sup> Computer Science and Software Engineering, Concordia University, Canada

<sup>3</sup> Computer Science and Computer Engineering, University of Arkansas, USA

ttdat@selab.hcmus.edu.vn, dcnhan@ieee.org, khoaluu@uark.edu, tmtriet@fit.hcmus.edu.vn

## Abstract

Recognition across domains has recently become an active topic in the research community. However, it has been largely overlooked in the problem of recognition in new unseen domains. Under this condition, the delivered deep network models are unable to be updated, adapted or fine-tuned. Therefore, recent deep learning techniques, such as: domain adaptation, feature transferring, and fine-tuning, cannot be applied. This paper presents a novel approach to the problem of domain generalization in the context of deep learning. The proposed method<sup>1</sup> is evaluated on different datasets in various problems, i.e. (i) digit recognition on MNIST, SVHN and MNIST-M, (ii) face recognition on Extended Yale-B, CMU-PIE and CMU-MPIE, and (iii) pedestrian recognition on RGB and Thermal image datasets. The experimental results show that our proposed method consistently improves the performance accuracy. It can be also easily incorporated with any other CNN frameworks within an end-to-end deep network design for object detection and recognition problems to improve their performance.

## 1. Introduction

Deep learning-based detection and recognition studies have been recently achieving very accurate performance in visual applications. However, many such methods assume the testing images come from the same distribution as the training ones, and often fail when performing in new unseen domains. Indeed, detection and classification crossing domains have recently become active topics in the research communities. In particular, *domain adaptation* [2, 26] has received significant attention in computer vision. In the domain adaptation (Fig. 1(A)), we usually have a large-scale

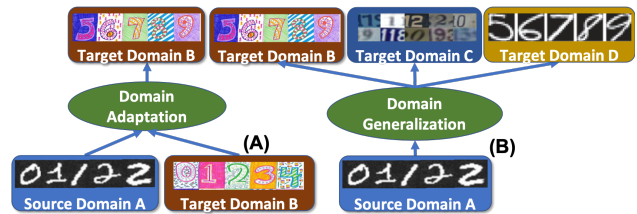


Figure 1: Comparison between Domain Adaptation (A) and our proposed Domain Generalization (B) problems

training set with labels, i.e. the source domain A, and a small training set with or without labels, i.e. the target domain B. The knowledge from the source domain A will be learned and adapted to the target domain B. During the testing time, the trained model will be deployed *only* in the target domain B. Recent results in domain adaptation have showed significant improvement in the many computer vision applications. However, the trained models are potentially deployed not only in the target domain B but also in many other *new unseen* domains, e.g. C, D, etc. (Fig. 1(B)) in real-world applications. In this scenarios, the released deep network models are usually unable to be retrained or fine-tuned with the inputs in new unseen domains or environments as illustrated in Fig. 2. Thus, domain adaptation cannot be applied in these problems since the new unseen target domains are unavailable.

Besides, there are some prior works to perform recognition problems with high accuracy by presenting new loss functions [20, 31] or increasing deep network structures [6] via mining hard samples in training sets. These loss functions are deployed to deal with hard samples considered as unseen domains. However, these methods are limited to be generalized in new unseen domains in real world applications. Some real world problems are unable to observe training samples from new unseen domains in the train-

<sup>1</sup>Source code will be publicly available.



Figure 2: The ideas of domain generalization. The deep model is trained only in a single domain (A), i.e. RGB images. It is deployed in other unseen domains, i.e. thermal images (B) and infrared images (C).

ing process. Therefore, in the scope of this work, there is no assumption about the new unseen domains. Our proposed method can be supportively incorporated with Convolutional Neural Networks (CNNs)-based detection and classification methods to train within an end-to-end deep learning framework to potentially improve the performance.

### 1.1. Contributions of this Work

This work presents a novel approach to domain generalization that can learn to better generalize new unseen domains. The restrictive setting is considered in this work where there is *only single source domain available for training*. Table 1 summarizes the differences between our approach and the prior works. Our contributions can be summarized as follows.

A novel approach named *Universal Non-volume Preserving (UNVP)* and its extension named *Extended Universal Non-volume Preserving (E-UNVP)* frameworks are firstly introduced to generalize environments of new unseen domains from a given single source training domain. Secondly, the environmental features extracted from the environment modeling via Deep Generative Flows (DGF) and the discriminative features extracted from the deep network classifiers are then unified together to provide a final generalized deep features that are robustly discriminative in new unseen domains. The proposed approach is designed and implemented within an end-to-end deep learning framework and inherits the power of the CNNs. It can be easily end-to-end integrated with a CNN-based deep network design for object detection or recognition to improve the performance. Finally, the proposed method is experimented in various visual modalities and applications with consistently improving performances.

## 2. Related Work

**Domain Adaptation** has recently become one of the most popular research topics in the field [2, 25, 21, 28, 26].

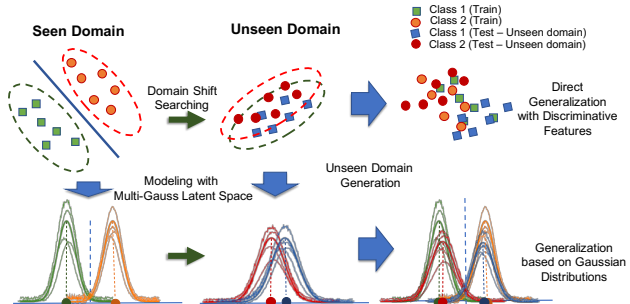


Figure 3: Illustration of the proposed UNVP method. The traditional classifier fails to model new samples in unseen domains (top). Meanwhile, UNVP consistently maintains the feature distribution in each class while searching for a new shifting domain (bottom).

Ganin et al. [2] proposed to incorporate both classification and domain adaptation to a unified network so that both tasks can be learned together. Similarly, Tzeng et al. [26] later introduced a unified framework for Unsupervised Domain Adaptation based on adversarial learning objectives (ADDA). It uses a loss function in a discriminator to be solely dependent on its target distribution. Liu et al. [13] presented Coupled Generative Adversarial Network (CoGAN) for learning a joint distribution of multi-domain images. It is then applied to domain adaptation.

**Domain Generalization** aims to learn a classification model from single source domain and generalize that knowledge to robustly achieve high performance in unseen target domains. In order to learn a domain-invariant feature representation, M. Ghifary et al. [4] used multi-view autoencoders to perform cross domain reconstructions. Later, [11] introduced MMD-AAE to learn a feature representation by jointly optimizing a multi-domain autoencoder regularized via the Maximum Mean Discrepancy (MMD) distance. Recently, K. Muandet et al. [14] presented a kernel-based algorithm for minimizing the differences in the marginal distributions of multiple domains whereas Y. Li [12] proposed an end-to-end conditional invariant deep domain generalization approach by leveraging deep neural networks for domain-invariant representation learning. To address the problem of unseen domains, R. Volpi et al. presented Adversarial Data Augmentation (ADA) [29] to generalize to unseen domains.

## 3. The Proposed Method

Far apart from previous augmentation methods that tried to generate new samples in image space using prior knowledge with the hope that these samples can cover unseen domains; our approach, on the other hand, focuses on modeling the environment density as multiple Gaussian distributions in a deep feature space and uses these knowledge

Table 1: Comparison in the properties between our proposed approaches (UNVP and E-UNVP) and other recent methods, where  $\times$  represents *not applicable* properties. Gaussian Mixture Model (GMM), Probabilistic Graphical Model (PGM), Convolutional Neural Network (CNN), Adversarial Loss ( $\ell_{adv}$ ), Log Likelihood Loss ( $\ell_{LL}$ ), Cycle Consistency Loss ( $\ell_{cyc}$ ), Discrepancy Loss ( $\ell_{dis}$ ) and Cross-Entropy Loss ( $\ell_{CE}$ ).

	Domain Modality	Architecture	Loss Function	End-to-End	Target-domain sample-free	Target-domain label-free	Deployable Domains
FT [30]	Transfer Learning	CNN	$\ell_2$	✓	✗	✗	Two
UBM [18]	Adaptation	GMM	$\ell_{LL}$	✗	✗	✓	Any
DANN [2]	Adaptation	CNN	$\ell_{adv}$	✓	✗	✓	Two
CoGAN [13]	Adaptation	CNN+GAN	$\ell_{adv}$	✓	✗	✓	Two
I2IAdapt [15]	Adaptation	CNN+GAN	$\ell_{adv} + \ell_{cyc}$	✓	✗	✓	Two
ADDA [27]	Adaptation	CNN+GAN	$\ell_{adv}$	✓	✗	✓	Two
MCD [19]	Adaptation	CNN+GAN	$\ell_{adv} + \ell_{dis}$	✓	✗	✓	Two
CrossGrad [22]	Generalization	Bayesian Net	$\ell_{CE}$	✓	✓	✓	Any
ADA [29]	Generalization	CNN	$\ell_{CE}$	✓	✓	✓	Any
<b>Our UNVP</b>	<b>Generalization</b>	<b>PGM+CNN</b>	$\ell_{LL} + \ell_{CE}$	✓	✓	✓	<b>Any</b>
<b>Our E-UNVP</b>	<b>Generalization</b>	<b>PGM+CNN</b>	$\ell_{LL} + \ell_{CE}$	✓	✓	✓	<b>Any</b>

for generalization process. By this way, the new samples are automatically synthesized with more semantic meaning while consistently maintaining the feature structures (see Fig. 3). As the result, without the need of seeing the samples in target domains, our proposed approach is still able to handle the domain shifting effectively and robustly achieves high performance in these unseen domains.

In particular, the proposed UNVP and E-UNVP approaches present a new *tractable CNN deep network* to extract the deep features of samples in the source environment and formulate their probability densities to *multiple Gaussian* distributions (Fig. 3). From these learned distributions, a density-based augmentation approach is employed to expand data distributions of the source environment for generalizing to different unseen domains. This architecture design allows to unify deep feature modeling and distribution modeling within an end-to-end framework as in Fig. 4.

The proposed framework consists of two main streams: (1) Discriminative feature modeling with a deep network classifier; and (2) Deep Generative Flows to model the domain variations in the form of distributions. They are together go through an end-to-end learning process that alternatively minimizes the within-class distributions and synthesizing new useful samples to generalize to new unseen domains. Notice that our proposed framework does not require the present of samples in the target domains during the training process.

### 3.1. Domain Variation Modeling as Distributions

This section aims at learning a Deep Generative Flow model, i.e. function  $\mathcal{F}$ , that maps an image  $\mathbf{x}$  in image space  $\mathcal{I}$  to its latent representation  $\mathbf{z}$  in latent domain  $\mathcal{Z}$  such that the density function  $p_X(\mathbf{x})$  can be estimated via the probability density function  $p_Z(\mathbf{z})$ . Then via  $\mathcal{F}$ , rather than representing

the environment variation, i.e.  $p_X(\mathbf{x})$ , directly in the image space, it can be easily modeled via variables in latent space, i.e.  $p_Z(\mathbf{z})$ , with more semantic manner. Moreover, when  $p_Z(\mathbf{z})$  follows some prior distributions, all samples in the given domain can be effectively modeled in the forms of latent distributions.

**Structure and Variable Relationship.** Let  $\mathbf{x} \in \mathcal{I}$  be a data sample in image domain  $\mathcal{I}$ ,  $y$  be its corresponding class label, and  $\mathbf{z} = \mathcal{F}(\mathbf{x}, y, \theta)$  where  $\theta$  denotes the parameters of  $\mathcal{F}$ , the probability density function of  $\mathbf{x}$  can be formulated via the change of variable formula as follows:

$$p_X(\mathbf{x}, y; \theta) = p_Z(\mathbf{z}, y; \theta) \left| \frac{\partial \mathcal{F}(\mathbf{z}, y; \theta)}{\partial \mathbf{x}} \right| \quad (1)$$

where  $p_X(\mathbf{x}, y)$  and  $p_Z(\mathbf{z}, y; \theta)$  define the distributions of samples of class  $y$  in image and latent domains, respectively.  $\frac{\partial \mathcal{F}(\mathbf{z}, y; \theta)}{\partial \mathbf{x}}$  denotes the Jacobian matrix with respect to  $\mathbf{x}$ . Then the log-likelihood is computed by.

$$\log p_X(\mathbf{x}, y; \theta) = \log p_Z(\mathbf{z}, y; \theta) + \log \left| \frac{\partial \mathcal{F}(\mathbf{z}, y; \theta)}{\partial \mathbf{x}} \right| \quad (2)$$

Eqns. (1) and (2) have provided two facts: (1) learning the density function of samples in class  $y$  is equivalent to estimate the density of its latent representation  $\mathbf{z}$  and determinant of the associated Jacobian matrix  $\frac{\partial \mathcal{F}}{\partial \mathbf{x}}$ ; and (2) if the latent distribution  $p_Z$  is defined as a Gaussian distribution, the learned function  $\mathcal{F}$  explicitly becomes the mapping function from a real data distribution to a Gaussian distribution in latent space. Then, we can model the environment variation via deviations from the Gaussian distributions of all classes in latent domain. Furthermore, when  $\mathcal{F}$  is well-defined with tractable computation of its Jacobian determinant, the two-way connection (i.e. inference and generation) can be established between  $\mathbf{x}$  and  $\mathbf{z}$ .

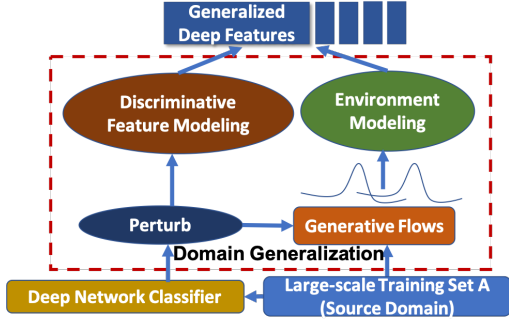


Figure 4: The Proposed Method.

**The prior class distributions.** Motivated from these properties, given  $C$  classes, we choose  $C$  Gaussian distributions with different means  $\{\mu_1, \mu_2, \dots, \mu_C\}$  and covariances  $\{\Sigma_1, \Sigma_2, \dots, \Sigma_C\}$  as prior distributions for these classes, i.e.  $\mathbf{z}_c \sim \mathcal{N}(\mu_c, \Sigma_c)$ . It is worth to note that even Gaussian Distributions are chosen, our framework is not limited to other distribution types.

**Mapping function structure.** In order to enforce the information flow from image domain to latent space with different abstraction levels, the mapping function  $\mathcal{F}$  is formulated as a composition of several sub-functions  $f_i$  as follows.

$$\mathcal{F} = f_1 \circ f_2 \circ \dots \circ f_N \quad (3)$$

where  $N$  is the number of sub-functions. The Jacobian  $\frac{\partial \mathcal{F}}{\partial \mathbf{x}}$  can be derived by  $\frac{\partial \mathcal{F}}{\partial \mathbf{x}} = \frac{\partial f_1}{\partial \mathbf{x}} \cdot \frac{\partial f_2}{\partial f_1} \dots \frac{\partial f_N}{\partial f_{N-1}}$ . With this structure, the properties of each  $f_i$  will define the properties for the whole mapping function  $\mathcal{F}$ . For example, if the Jacobian of  $\frac{\partial f_1}{\partial \mathbf{x}}$  is tractable, then  $\mathcal{F}$  is also tractable. Furthermore, if  $f_i$  is a non-linear function built from a composition of CNN layers then  $\mathcal{F}$  becomes a deep convolution neural network. There are several ways to construct the sub-functions, i.e. borrowing different CNN structures for non-linearity property. In our approach, the sub-function in [17] is adopted thanks to its tractable and invertible.

$$f(\mathbf{x}) = \mathbf{b} \odot \mathbf{x} + (1 - \mathbf{b}) \odot [\mathbf{x} \odot \exp(\mathcal{S}(\mathbf{b} \odot \mathbf{x}) + \mathcal{T}(\mathbf{b} \odot \mathbf{x}))] \quad (4)$$

where  $\mathbf{b} = [1, \dots, 1, 0, \dots, 0]$  is a binary mask, and  $\odot$  is the Hadamard product.  $\mathcal{S}$  and  $\mathcal{T}$  define the scale and translation functions during mapping process.

**Learning the mapping function and Environment Modeling.** In order to learn the parameter  $\theta$  for mapping function  $\mathcal{F}$ , the log-likelihood in Eqn. (2) is maximized as follows.

$$\theta^* = \arg \max_{\theta} \sum_c \sum_i \log p_X(\mathbf{x}^i, c; \theta) \quad (5)$$

Notice that after learning the mapping function, **all images of all classes are mapped into the corresponding distributions of their classes**. Then the environment density

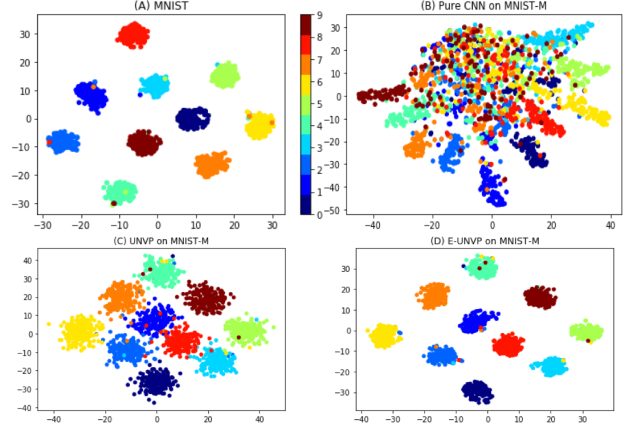


Figure 5: The distributions: (A) Distribution of samples in MNIST. (B) Distribution of MNIST-M using a Pure-CNN trained on MNIST, (C) Distribution of MNIST-M using our UNVP trained on MNIST. (D) Distribution of MNIST-M using our E-UNVP trained on MNIST.

can be considered as the composition of these distributions. Figure 5(A) illustrated an example of the learned environment distributions of MNIST with 10 digit classes. When only samples in MNIST are used for training, the density distributions of MNIST-M, i.e. *unseen during training*, using Pure-CNN, our UNVP and E-UNVP are shown in Fig. 5 (B, C, D), respectively. In next section, a generalization approach is proposed so that using only samples in source environment, the learned model can expand the density distributions of source environment so that they can cover as much as possible the distributions of unseen environments.

### 3.2. Unseen Domain Generalization

After modeling the source environment variation as the compositions of its class distributions, this section introduces the generalization process of these distributions with respect to a classification model  $\mathcal{M}$  such that the expansion of these distributions can help  $\mathcal{M}$  generalize to unseen environments with high accuracy. Notice that  $\mathcal{M}$  can be any type of Deep CNN such as LeNet [10], AlexNet [9], VGG [24], ResNet [1], DenseNet [7].

Let  $\ell(\mathbf{X}, \mathbf{Y}; \mathcal{M}, \mathcal{F}, \theta, \theta_1)$  be the training loss function of  $\mathcal{M}$ , and  $\theta_1$  be the parameters of  $\mathcal{M}$ . The generalization process of  $\mathcal{M}$  can be formulated as updating the parameters  $\theta_1$  such that it can robustly classify the samples having latent distributions that are distance  $\rho$  away from the samples in the source environment. Then, the objective function of  $\mathcal{M}$  is formulated as.

$$\arg \min_{\theta_1} \sup_{P: d(P_X, P_X^{src}) \leq \rho} \mathbb{E}[\ell(\mathbf{X}, \mathbf{Y}; \mathcal{M}, \mathcal{F}, \theta, \theta_1)] \quad (6)$$

where  $\{\mathbf{X}, \mathbf{Y}\}$  denotes the images and their labels;  $d(\cdot, \cdot)$  is the distance between probability distributions;  $P_X^{src}(\mathbf{X}, \mathbf{Y})$

and  $P_X(\mathbf{X}, \mathbf{Y})$  are the density distributions of the source and current expanded environments, respectively.

Since both  $P_X^{src}$  and  $P_X$  are density distributions, the Wasserstein distance with respect to  $P_X^{src}$  and  $P_X$  can be adopted. Notice that from previous section, we have learned a mapping function  $\mathcal{F}$  that maps the density functions from image space, i.e.  $P_X$ , to prior distributions in latent space, i.e.  $P_Z$ . Moreover, since  $\mathcal{F}$  is invertible with the specific formula of its sub-functions, computing  $d(P_X, P_X^{src})$  is equivalent to  $d(P_Z, P_Z^{src})$ . From this, we can efficiently estimate  $cost$  as the transformation cost between Gaussian distributions. Then  $d(P_X, P_X^{src})$  is reformulated by.

$$\begin{aligned} d(P_X, P_X^{src}) &= d(P_Z, P_Z^{src}) \\ &= \sum_c \sum_{\mathbf{x}_c, \mathbf{x}_c^{src}} \inf \mathbb{E} [cost(\mathcal{F}(\mathbf{x}_c), \mathcal{F}(\mathbf{x}_c^{src}))] \\ &= \sum_c \sum_{\mathbf{z}_c, \mathbf{z}_c^{src}} \inf \mathbb{E} [cost(\mathbf{z}_c, \mathbf{z}_c^{src})] \end{aligned} \quad (7)$$

where  $cost(\cdot, \cdot)$  denotes the transformation cost between Gaussian distributions:

$$\begin{aligned} cost^2(\mathbf{z}_c, \mathbf{z}_c^{src}) &= \sum_c \|\mu_c^{src} - \mu_c\|_2^2 \\ &+ \text{Tr}(\Sigma_c^{src} + \Sigma_c - 2((\Sigma_c^{src})^{1/2} \Sigma_c (\Sigma_c^{src})^{1/2})^{1/2}) \end{aligned} \quad (8)$$

$\{\mu_c, \Sigma_c\}$  and  $\{\mu_c', \Sigma_c'\}$  are the means and covariances of the distributions of class  $c$  in the source and the expanded environment, respectively. Plugging this distance and applying the Lagrangian relaxation to Eqn. (6), we have

$$\begin{aligned} &\arg \min_{\theta_1} \sup_P \mathbb{E} [\ell(\mathbf{X}, \mathbf{Y}; \mathcal{M}, \mathcal{F}, \theta, \theta_1)] - \alpha \cdot d(P_X, P_X^{src}) \\ &= \arg \min_{\theta_1} \sum_c \sup_{\mathbf{x}} \{\ell(\mathbf{x}, c; \mathcal{M}, \mathcal{F}, \theta, \theta_1) - \alpha \cdot cost(\mathcal{F}(\mathbf{x}), \mathcal{F}(\mathbf{x}_c^{src}))\} \end{aligned} \quad (9)$$

To solve this objective function, the optimization process can be divided into two alternative steps: (1) generate the sample  $\mathbf{x}$  for each class such that

$$\mathbf{x} = \arg \max_{\mathbf{x}} \{\ell(\mathbf{x}, c; \mathcal{M}, \mathcal{F}, \theta, \theta_1) - \alpha \cdot cost(\mathcal{F}(\mathbf{x}), \mathcal{F}(\mathbf{x}_c^{src}))\} \quad (10)$$

and consider  $\mathbf{x}$  as a new ‘‘hard’’ example for class  $c$ ; and (2) add  $\mathbf{x}$  to the training data and optimize the model  $\mathcal{M}$ . In other words, this two-step optimization process aims at finding new samples belonging to distributions that are  $\rho$  distance far away from the distributions of the source environment, and making  $\mathcal{M}$  become more robust when classifying these examples. By this way, after a certain of iteration, the distributions learned from  $\mathcal{M}$  can be generalized so that they can cover as much as possible the distributions of new unseen environments.

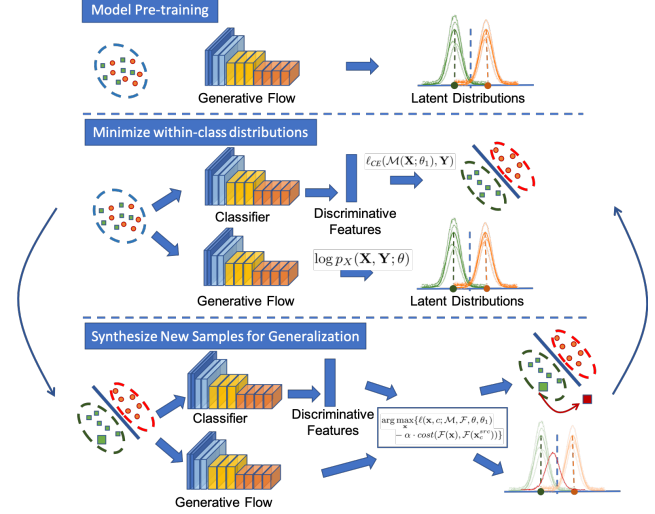


Figure 6: **The Training Process of Our proposed UNVP** consists of one pre-training step and a two-stage optimization by alternatively minimizing the within-class distributions and synthesizing new samples for generalization.

### 3.3. Universal Non-volume Preserving (UNVP) Models

The proposed UNVP consists of two main branches: (1) *Discriminative Feature Modeling* and (2) *Generative Distribution Modeling*. While the discriminative part focuses on constructing a classifier that minimizes within-class distributions, the generative one aims at embedding samples of all classes into their corresponding latent distributions and then expanding these distributions for generalization. The whole end-to-end joint training process for UNVP is illustrated in Fig. 6 where the generative part of UNVP (i.e. *Deep Generative Flow*  $\mathcal{F}$ ) is firstly employed to learn the mapping from image space to Gaussian distributions in latent space. Then a two-stage training process is adopted to learn the Deep Classifier  $\mathcal{M}$  and adjust the Deep Generative Flow  $\mathcal{F}$  for generalization.

In the first stage of this process, given a training dataset, both parameters  $\{\theta, \theta_1\}$  of the mapping function  $\mathcal{F}$  and the classifier  $\mathcal{M}$  are updated according to the loss function as.

$$\ell(\mathbf{X}, \mathbf{Y}; \mathcal{M}, \mathcal{F}, \theta, \theta_1) = \ell_{CE}(\mathcal{M}(\mathbf{X}; \theta_1), \mathbf{Y}) - \log p_X(\mathbf{X}, \mathbf{Y}; \theta) \quad (11)$$

where the first term is the cross-entropy loss for  $\mathcal{M}$  and the second term is the log-likelihood of  $\mathcal{F}$ .

In the second stage, we adapt the generalization process as presented in Sec. 3.2 and Eqn. (10) to synthesize new ‘‘hard’’ samples. Notice that, to further constraint the perturbation in latent space, we incorporate another regular-

ization term to Eqn. (7) as.

$$\begin{aligned} cost^2(\mathbf{z}_c, \mathbf{z}_c^{src}) &= \sum_c \|\mu_c^{src} - \mu_c\|_2^2 \\ &+ \text{Tr}(\Sigma_c^{src} + \Sigma_c - 2((\Sigma_c^{src})^{1/2} \Sigma_c (\Sigma_c^{src})^{1/2})^{1/2}) \\ &+ \|\mathcal{M}(\mathbf{X}_c) - \mathcal{M}(\mathbf{X}_c^{src})\|_2^2 \end{aligned}$$

New generated samples are then added to the training set and used for updating both branches of UNVP.

Notice that in the structure of  $\mathcal{F}$ , the choice of Gaussian distributions for all classes play an important role and directly affects the performance of the generative model. By varying the choices for these distributions, different variants of UNVP can be introduced.

#### Universal Non-volume Preserving Models (UNVP):

The means and covariances of Gaussian distributions are pre-defined for all  $C$  classes where  $\mu_c = \mathbf{1}_c$ ;  $\Sigma = \mathbf{I}$ ;  $\mathbf{z}_c \sim \mathcal{N}(\mu_c, \mathbf{I})$  where  $\mathbf{1}$  is the all-one vector.

#### Extended Universal Non-volume Preserving Models (E-UNVP):

Rather than fixing the means and covariances of the Gaussian distributions of  $C$  classes, they are considered as variables and flexibly learned during the environment modeling as well as adjusted during domain generalization. Particularly, given the class label  $c$ ,  $\mathcal{F}$  maps each sample  $\mathbf{x}_c$  to a Gaussian distribution with the mean and covariance as.

$$\begin{aligned} \mu_c &= \gamma \mathcal{G}_m(c) + \lambda \mathcal{H}_m(\mathbf{n}) \\ \Sigma_c &= \mathcal{G}_{std}(c) \end{aligned} \quad (12)$$

where  $\mathcal{G}_m(c)$  and  $\mathcal{G}_{std}(c)$  denote the learnable function that map label  $c$  to the mean and covariance values of its Gaussian distribution.  $\mathbf{n}$  is a noise signal that is generated following the normal distribution.  $\mathcal{H}_m(\mathbf{n})$  defines the allowable shifting range of the Gaussian given the noise signal  $\mathbf{n}$ .  $\gamma$  and  $\lambda$  are user-defined parameters that control the separation of the Gaussian Distributions between different classes and the contribution of  $\mathcal{H}_m(\mathbf{n})$  to  $\mu_c$ . We choose the Fully Connected structure for  $\mathcal{G}_m(c)$  and  $\mathcal{G}_{std}(c)$  that take the input  $c$  in the form of one-hot vector while Convolutional Layer is adopted for  $\mathcal{H}_m(\mathbf{n})$ .

## 4. Discussion

As shown in Fig. 3, by exploiting the Generative Flows that model samples of each class as a Gaussian in semantic feature space, the proposed UNVP can robustly maintain the feature structure of each class during expanding and shifting the domain distributions. This helps to generate more useful ‘‘hard’’ samples for the generalization process.

By introducing the noise signal  $\mathbf{n}$ , we allow the Gaussian distribution of each class shifting around within a limited range, i.e.  $\mathcal{H}_m(\mathbf{n})$ . This further enhances the robustness of E-UNVP against noise during the environment modeling.



Figure 7: Examples in (A) MNIST, (B) MNIST-M, and (C) SVHN databases

To further enhance the capability of modeling the input signal with high-resolution, we incorporate the activation normalization and invertible  $1 \times 1$  convolution operators [8] to the structure of each sub-function  $f_i$  in Eqn. (3). Particularly, the input to each  $f_i$  is passed through an actnorm layer followed by an invertible  $1 \times 1$  convolution before being transformed by  $\mathcal{S}$  and  $\mathcal{T}$  as in Eqn. (4). The two transformations  $\mathcal{S}$  and  $\mathcal{T}$  are defined by two Residual Networks with rectifier non-linearity and skip connections. Each of them contains three residual blocks. For input image with the resolution higher than  $128 \times 128$ , six residual blocks are set for  $\mathcal{S}$  and  $\mathcal{T}$ .

## 5. Experiments

This section first shows the effectiveness of our proposed methods with comprehensive ablative experiments in Sec. 5.1. In these experiments, MNIST is used as *the only* training set and MNIST-M is used as the unseen testing set. The proposed approaches are also benchmarked on various deep network structures, i.e. LeNet [10], AlexNet [9], VGG [24], ResNet [1] and DenseNet [7]. Using the final optimal model, Sec. 5.2 shows our approaches consistently achieve the state-of-the-art results in digit recognition on three digit datasets, i.e. MNIST, SVHN [16] and MNIST-M. Sec. 5.3 shows the proposed approaches in face recognition in three databases, i.e. Extended Yale-B [3], CMU-PIE [23] and CMU-MPIE [5]. Facial images with normal illumination are used as the training domain and the ones in dark illumination conditions are used as the testing set on the new unseen domains (Fig. 8). Finally, we show the advantages of UNVP and E-UNVP in the cross-domain pedestrian recognition on the Thermal Database in Sec. 5.4.

### 5.1. Ablation Study

This experiment aims to measure the effectiveness of the domain generalization and perturbation processes (Fig. 4). This experiment uses MNIST as the only training set and MNIST-M as the testing one. In order to simplify the experiment, LeNet [10] is used as the classifier, i.e. Pure-CNN. About the network hyper-parameters, the learning rate and the batch size are set to 0.0001 and 128, respectively.

**Hyper-parameter Settings.** In Generative Flows Learning process, the multiple Gaussian distributions are handled

Table 2: Ablative experiment results (%) on effectiveness of the parameters  $\lambda$ ,  $\alpha$  and  $\beta$  that control the distribution separation and shifting range. MNIST is used as the only training set, MNIST-M is used as the unseen testing set.

Dataset	Methods	$\lambda$			$\alpha$			$\beta(\%)$				
		0.01	0.1	1.0	0.01	0.1	1.0	0%	1%	10%	20%	30%
MNIST	Pure-CNN	99.28										
	UNVP	–	–	–	<b>99.33</b>	99.18	99.30	99.28	99.28	<b>99.35</b>	99.30	99.36
	E-UNVP	<b>99.22</b>	<b>99.42</b>	<b>99.40</b>	99.13	<b>99.31</b>	<b>99.42</b>	<b>99.28</b>	<b>99.36</b>	99.34	<b>99.42</b>	<b>99.43</b>
MNIST-M	Pure-CNN	55.90										
	UNVP	–	–	–	<b>58.18</b>	60.76	59.44	55.90	<b>59.99</b>	57.24	59.44	55.11
	E-UNVP	<b>59.83</b>	<b>60.49</b>	<b>59.47</b>	56.92	<b>61.70</b>	<b>60.49</b>	<b>55.90</b>	57.10	<b>60.49</b>	<b>61.70</b>	<b>60.49</b>

by the set of scale parameters, i.e.  $\gamma$  and  $\lambda$ , to control the distribution separation and shifting range as shown in Eqn. (12). The contributions of the generalization process are also evaluated with various percentage of “hard” generated samples ( $\beta$ ), i.e. from 0% to 30%. When  $\beta = 0$ , no new samples are not generated.

There are two phases alternatively updated in the training process: (1) Minimization phase to optimize the networks and (2) Maximization (perturb) phase to generate new hard examples. We do  $K$  times of the maximization phase, for each time, we randomly select  $\beta$  percent of the number of training images to generate new hard samples via deep generative models. Specifically, our maximization phase generalizes new images based on both semantic features from the CNN classifier and the semantic space via the estimation of environment density. The experimental results in Table 2 show that the proposed approaches consistently help to improve the classifiers.

**Sample Distributions in Unseen Domains.** The sample class distributions with the optimal parameter set are used to visually observed and demonstrated as in Fig. 5. While Pure-CNN obviously fails to model unseen domain MNIST-M dataset, our UNVP successfully does domain shift and cover unseen domain dataset. These sample distributions are completely class separated when using our E-UNVP.

**Backbone Deep Networks.** This section evaluates the robustness and the consistent improvements of UNVP and E-UNVP with common deep networks, including LeNet, AlexNet, VGG, ResNet and DenseNet as in Table 3. The proposed UNVP and E-UNVP consistently outperform the stand-alone classifier (Pure-CNN) using the same network configuration in all experiments. Particularly, it helps to improve **6%**, **0.5%**, **4%**, **5%**, **2%** on MNIST-M using LeNet, AlexNet, VGG, ResNet and DenseNet respectively.

The proposed methods can be easily integrated with standard CNN deep networks. Therefore, it potentially can be applied to improve the performance in many existed CNN-based applications, e.g detection and recognition, that are experimented in the next sections.

Table 3: Experimental results (%) when using UNVP and E-UNVP in various common CNNs.

Networks	Methods	MNIST	MNIST-M
LeNet	Pure-CNN	99.06	55.90
	UNVP	99.30	59.44
	E-UNVP	<b>99.42</b>	<b>61.70</b>
AlexNet	Pure CNN	<b>99.17</b>	40.12
	UNVP	98.81	39.94
	E-UNVP	98.89	<b>40.60</b>
VGG	Pure CNN	99.43	50.67
	UNVP	<b>99.42</b>	<b>54.41</b>
	E-UNVP	99.40	51.37
ResNet	Pure CNN	98.01	35.35
	UNVP	98.82	37.15
	E-UNVP	<b>98.97</b>	<b>40.60</b>
DenseNet	Pure CNN	99.23	41.16
	UNVP	<b>99.42</b>	41.98
	E-UNVP	99.14	<b>43.72</b>

Table 4: Experimental results (%) on three digit datasets. ADA and our approaches **do not require** target domain data in training. ADDA, DANN **require** training data from target domains during training steps.

Methods	MNIST	SVHN	MNIST-M
ADDA	99.29	32.20	63.39
DANN	–	–	76.66
Pure-CNN	99.06	31.96	55.90
ADA	99.17	37.87	60.02
UNVP	99.30	41.23	59.45
E-UNVP	<b>99.42</b>	<b>42.87</b>	<b>61.70</b>

## 5.2. Digit Recognition on Unseen Domains

The proposed approaches are experimented in digit recognition on new unseen domains with two other digit databases, i.e. MNIST-M and SVHN (Fig. 7). In this experiment, MNIST is the only database used to train the classifier. Then, two other datasets, i.e. MNIST-M and SVHN



Figure 8: Examples of Yale-B [3] and CMU-PIE [23] databases. Face images in normal illumination (N) (the 1st row) are used as training domain and the ones in dark illumination (D) (the 2nd row) are used for testing.

Table 5: Experimental results (%) on Extended Yale-B [3], CMU-PIE [23] and CMU-MPIE [5] databases. It is notice that ADA and our proposed approaches **do not require** target domain data during training while ADDA **does**.

Method	E-Yale-B		CMU-PIE		CMU-MPIE	
	N	D	N	D	N	D
ADDA	99.17	75.28	96.09	70.33	99.93	97.71
Pure-CNN	98.50	51.39	95.59	62.18	99.93	94.74
ADA	99.00	53.08	96.49	62.69	99.92	96.08
UNVP	99.17	58.24	96.32	64.88	99.83	<b>98.25</b>
E-UNVP	<b>99.54</b>	<b>62.95</b>	<b>97.55</b>	<b>66.89</b>	<b>99.93</b>	98.03

are used as the new unseen domains to benchmark the performance. The classifier is trained using 50,000 images of MNIST. In order to generalizing new image phase, we use 10,000 images in this set to perturb and generalize new samples. All digit images are resized to  $32 \times 32$ .

The learned classifiers are then benchmarked on MNIST and two other unseen digit datasets, i.e. SVHN and MNIST-M. The classification results using the proposed approach are compared against the LeNet classifier (Pure-CNN), and the Adversarial Data Augmentation (ADA). We also show the recognition results on these datasets using the Domain Adaptation methods, including: Adversarial Discriminative Domain Adaptation (ADDA), Domain-Adversarial Training of Neural Networks (DANN) [2]. It is noticed that Pure-CNN, ADA and our approaches do not require the target domain data during training. Meanwhile, ADDA, DANN require the target domain data in the training steps.

Our generalization phase synthesizes images based on semantic space via the estimation of environment density. It helps our generated images to be more diverse than the synthesized images using ADA method. The experimental results are shown in Table 4. The proposed methods consistently achieve the state-of-the-art performance on these datasets. Particularly, it helps to improve approximately **11%** and **6%** on SVHN and MNIST-M, respectively.

### 5.3. Face Recognition on Unseen Domains

In this experiment, the proposed approaches are applied in unseen environment face recognition and compared against the other baseline methods, i.e. Pure-CNN, ADA

Table 6: Experimental results (%) on RGB and Thermal pedestrian databases with various common deep network structures.

Networks	Methods	RGB	Thermal
LeNet	Pure-CNN	95.45	79.72
	<b>E-UNVP</b>	<b>97.25</b>	<b>90.29</b>
AlexNet	Pure CNN	96.64	81.38
	<b>E-UNVP</b>	<b>97.04</b>	<b>82.98</b>
VGG	Pure CNN	97.54	95.60
	<b>E-UNVP</b>	<b>98.64</b>	<b>98.38</b>
ResNet	Pure CNN	98.52	96.07
	<b>E-UNVP</b>	<b>98.56</b>	<b>98.35</b>
DenseNet	Pure CNN	98.39	95.87
	<b>E-UNVP</b>	<b>98.60</b>	<b>96.14</b>

and ADDA, on three face recognition databases, including: Extended Yale-B, CMU-PIE and CMU-MPIE (Fig. 8). In each database, the face images with normal lighting are selected as the source domain, i.e. Normal illumination (N), and the face images with dark lighting are selected as the target domain, i.e. Dark illumination (D). Each database is randomly split into two sets: training set (80%) and testing set (20%). The experimental framework structures are similar to the one in digit recognition. All cropped face images are resized to  $64 \times 64$  pixels. The experimental results in Table 5 show that our proposed methods help to improve the recognition performance on new unseen domains where the lighting conditions are unknown. Particularly, it helps to improve approximately **11%**, **4%** and **3%** in dark lighting conditions on Extended Yale-B, CMU-PIE and CMU-MPIE databases respectively.

### 5.4. Pedestrian Recognition on Unseen Domains

This experiment aims to improve RGB-based pedestrian recognition on thermal images on the Thermal Dataset<sup>2</sup>. There are two datasets organized in this experiment: (1) RGB pedestrian and (2) Thermal pedestrian. The methods are trained only on the RGB pedestrian dataset and tested on the Thermal pedestrian dataset. In the training phase, we use 2,000 images to generalize new images, all images of two datasets are resized to  $128 \times 128$  pixels. The experimental results in Table 6 shows that our proposed methods consistently help to improve the performance of the Pure-CNN in various common deep network structures, including: LeNet, AlexNet, VGG, RestNet and DenseNet.

## 6. Conclusions

This paper has introduced the novel deep learning based domain generalization approach that generalizes well to dif-

<sup>2</sup><https://www.flir.com/oem/adas/adas-dataset-form/>



ferent unseen domains. Only using training data from a source domain, we propose an iterative procedure that augments the dataset with samples from a fictitious target domain that is hard under the current model. It can be easily integrated with any other CNN based framework within an end-to-end network to improve the performance. On digit recognition, the proposed method has been benchmarked on three popular digit recognition datasets and consistently showed the improvement. The method is also experimented in face recognition on three standard databases and outperforms the other state-of-the-art methods. In the problem of pedestrian recognition, we empirically observe that the proposed method learns models that improve performance across a priori unknown data distributions.

## References

- [1] *2016 IEEE Conference on Computer Vision and Pattern Recognition, CVPR 2016, Las Vegas, NV, USA, June 27-30, 2016*. IEEE Computer Society, 2016.
- [2] Y. Ganin and V. Lempitsky. Unsupervised domain adaptation by backpropagation. In F. Bach and D. Blei, editors, *Proceedings of the 32nd International Conference on Machine Learning*, volume 37 of *Proceedings of Machine Learning Research*, pages 1180–1189, Lille, France, 07–09 Jul 2015. PMLR.
- [3] A. Georghiades, P. Belhumeur, and D. Kriegman. From few to many: Illumination cone models for face recognition under variable lighting and pose. *IEEE Trans. Pattern Anal. Mach. Intelligence*, 23(6):643–660, 2001.
- [4] M. Ghifary, W. Bastiaan Kleijn, M. Zhang, and D. Balduzzi. Domain generalization for object recognition with multi-task autoencoders. In *The IEEE International Conference on Computer Vision (ICCV)*, December 2015.
- [5] R. Gross, I. Matthews, J. Cohn, T. Kanade, and S. Baker. Multi-pie. *Image Vision Comput.*, 28(5):807–813, May 2010.
- [6] G. Huang, Z. Liu, L. van der Maaten, and K. Q. Weinberger. Densely connected convolutional networks. In *The IEEE Conference on Computer Vision and Pattern Recognition (CVPR)*, July 2017.
- [7] G. Huang, Z. Liu, L. van der Maaten, and K. Q. Weinberger. Densely connected convolutional networks. In *Proceedings of the IEEE Conference on Computer Vision and Pattern Recognition*, 2017.
- [8] D. P. Kingma and P. Dhariwal. Glow: Generative flow with invertible 1x1 convolutions. In *Advances in Neural Information Processing Systems 31: Annual Conference on Neural Information Processing Systems 2018, NeurIPS 2018, 3-8 December 2018, Montréal, Canada.*, pages 10236–10245, 2018.
- [9] A. Krizhevsky, I. Sutskever, and G. E. Hinton. Imagenet classification with deep convolutional neural networks. In F. Pereira, C. J. C. Burges, L. Bottou, and K. Q. Weinberger, editors, *Advances in Neural Information Processing Systems 25*, pages 1097–1105. Curran Associates, Inc., 2012.
- [10] Y. Lecun, L. Bottou, Y. Bengio, and P. Haffner. Gradient-based learning applied to document recognition. *Proceedings of the IEEE*, 86(11):2278–2324, Nov. 1998.
- [11] H. Li, S. Jialin Pan, S. Wang, and A. C. Kot. Domain generalization with adversarial feature learning. In *The IEEE Conference on Computer Vision and Pattern Recognition (CVPR)*, June 2018.
- [12] Y. Li, X. Tian, M. Gong, Y. Liu, T. Liu, K. Zhang, and D. Tao. Deep domain generalization via conditional invariant adversarial networks. In *The European Conference on Computer Vision (ECCV)*, September 2018.
- [13] M.-Y. Liu and O. Tuzel. Coupled generative adversarial networks. In D. D. Lee, M. Sugiyama, U. V. Luxburg, I. Guyon, and R. Garnett, editors, *Advances in Neural Information Processing Systems 29*, pages 469–477. Curran Associates, Inc., 2016.
- [14] K. Muandet, D. Balduzzi, and B. Schölkopf. Domain generalization via invariant feature representation. In S. Dasgupta and D. McAllester, editors, *Proceedings of the 30th International Conference on Machine Learning*, volume 28 of *Proceedings of Machine Learning Research*, pages 10–18, Atlanta, Georgia, USA, 17–19 Jun 2013. PMLR.
- [15] Z. Murez, S. Kolouri, D. Kriegman, R. Ramamoorthi, and K. Kim. Image to image translation for domain adaptation. In *The IEEE Conference on Computer Vision and Pattern Recognition (CVPR)*, June 2018.
- [16] Y. Netzer, T. Wang, A. Coates, A. Bissacco, B. Wu, and A. Y. Ng. Reading digits in natural images with unsupervised feature learning. In *NIPS Workshop on Deep Learning and Unsupervised Feature Learning 2011*, 2011.
- [17] C. Nhan Duong, K. Gia Quach, K. Luu, N. Le, and M. Savvides. Temporal non-volume preserving approach to facial age-progression and age-invariant face recognition. In *The IEEE International Conference on Computer Vision (ICCV)*, Oct 2017.
- [18] D. A. Reynolds, T. F. Quatieri, and R. B. Dunn. Speaker verification using adapted gaussian mixture models. In *Digital Signal Processing*, page 2000, 2000.
- [19] K. Saito, K. Watanabe, Y. Ushiku, and T. Harada. Maximum classifier discrepancy for unsupervised domain adaptation. In *Proceedings of the IEEE Conference on Computer Vision and Pattern Recognition*, pages 3723–3732, 2018.
- [20] F. Schroff, D. Kalenichenko, and J. Philbin. Facenet: A unified embedding for face recognition and clustering. *CoRR*, abs/1503.03832, 2015.
- [21] O. Sener, H. O. Song, A. Saxena, and S. Savarese. Learning transferrable representations for unsupervised domain adaptation. In *Proceedings of the 30th International Conference on Neural Information Processing Systems, NIPS’16*, pages 2118–2126, USA, 2016. Curran Associates Inc.
- [22] S. Shankar, V. Piratla, S. Chakrabarti, S. Chaudhuri, P. Jyothi, and S. Sarawagi. Generalizing across domains via cross-gradient training. 2018.
- [23] T. Sim, S. Baker, and M. Bsat. The cmu pose, illumination, and expression (pie) database. In *Proceedings of the Fifth IEEE International Conference on Automatic Face and Gesture Recognition, FGR ’02*, pages 53–, Washington, DC, USA, 2002. IEEE Computer Society.

- [24] K. Simonyan and A. Zisserman. Very deep convolutional networks for large-scale image recognition. In *International Conference on Learning Representations*, 2015.
- [25] E. Tzeng, J. Hoffman, T. Darrell, and K. Saenko. Simultaneous deep transfer across domains and tasks. *CoRR*, abs/1510.02192, 2015.
- [26] E. Tzeng, J. Hoffman, K. Saenko, and T. Darrell. Adversarial discriminative domain adaptation. In *The IEEE Conference on Computer Vision and Pattern Recognition (CVPR)*, July 2017.
- [27] E. Tzeng, J. Hoffman, K. Saenko, and T. Darrell. Adversarial discriminative domain adaptation. *CoRR*, abs/1702.05464, 2017.
- [28] E. Tzeng, J. Hoffman, N. Zhang, K. Saenko, and T. Darrell. Deep domain confusion: Maximizing for domain invariance. *CoRR*, abs/1412.3474, 2014.
- [29] R. Volpi, H. Namkoong, O. Sener, J. C. Duchi, V. Murino, and S. Savarese. Generalizing to unseen domains via adversarial data augmentation. *CoRR*, abs/1805.12018, 2018.
- [30] X. Yin, X. Yu, K. Sohn, X. Liu, and M. Chandraker. Feature transfer learning for deep face recognition with long-tail data. *CoRR*, abs/1803.09014, 2018.
- [31] X. Zhang, Z. Fang, Y. Wen, Z. Li, and Y. Qiao. Range loss for deep face recognition with long-tail. *CoRR*, abs/1611.08976, 2016.